PROCEEDINGS OF SCIENCE

Recent results from the H1 experiment

Katja Krüger
Kirchhoff-Institut für Physik, Universität Heidelberg
E-mail: katja.krueger@desy.de

on behalf of the H1 Collaboration

An overview of recent results from the H1 collaboration is given. Measurements of the structure of the proton, of the hadronic final state and of diffractive processes as well as searches for physics beyond the Standard Model are presented.

XVIII International Workshop on Deep-Inelastic Scattering and Related Subjects, DIS 2010
April 19-23, 2010
Firenze, Italy

1. Introduction

The HERA ep collider in Hamburg was operated in the years 1992 to 2007, colliding electrons or positrons with an energy of 27.6 GeV and protons with an energy of 820/920 GeV, at a centre-of-mass energy of 304/319 GeV. During the HERA I running phase, until the year 2000, both collider experiments H1 and ZEUS collected a luminosity of about 120 pb^{-1} each. In the HERA II running phase, $\sim 380\,\mathrm{pb}^{-1}$ per experiment were recorded with polarised lepton beams. The last months of data taking were dedicated to special low energy runs, with proton energies of 460 and 575 GeV.

2. Proton Structure

Electron proton scattering at HERA offers a unique possibility to study the structure of the proton. In deep-inelastic scattering (DIS), the neutral current cross section as a function of the virtuality Q^2 of the exchanged boson and the Bjorken scaling variable x can be expressed in terms of structure functions:

$$\tilde{\sigma}^{\pm}_{\mathrm{NC}} = \frac{\mathrm{d}^2\sigma^{e^{\pm}p}_{\mathrm{NC}}}{\mathrm{d}x\mathrm{d}Q^2} \cdot \frac{Q^4 x}{2\pi\alpha^2 Y_+} = F_2(x,Q^2) \mp \frac{Y_-}{Y_+} xF_3(x,Q^2) - \frac{y^2}{Y_+} F_L(x,Q^2)\ ,$$

where $Y_{\pm} = 1 \pm (1-y)^2$ with the inelasticity y .

Especially the runs with reduced proton beam energy in the last three month of HERA operation allow a direct determination of the longitudinal proton structure function F_L by measuring the inclusive scattering cross section at fixed Q^2 and x for different y. Figure 1 (left) shows the measurement of F_L obtained from the combined cross section results from the H1 and ZEUS collaborations. The measurement agrees reasonably well with the expectation based on the HERAPDF1.0 set [1] of proton parton density functions (PDFs) extracted from the inclusive F_2 measurements at HERA I. These data are also included in a fit of the PDFs with the same parameterisations and

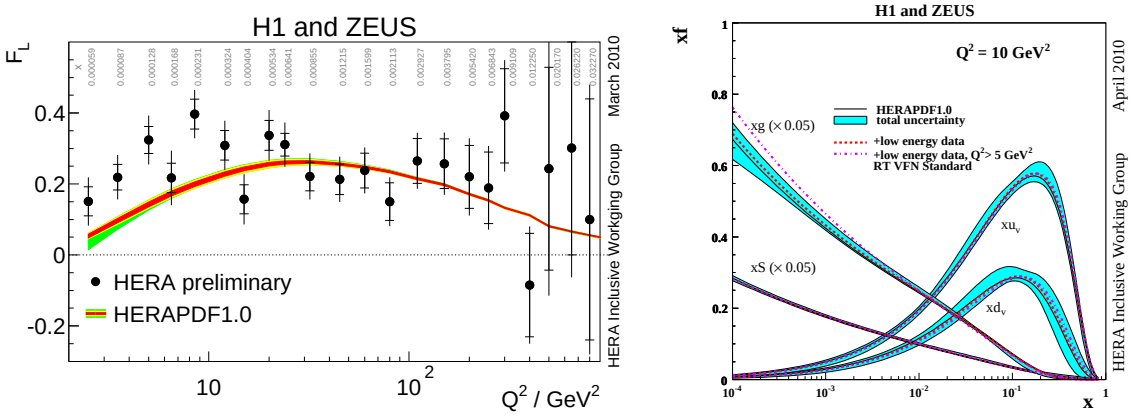

Figure 1: Longitudinal proton structure function F_L extracted from the combined H1+ZEUS inclusive cross sections at different proton beam energies (left). Proton PDF sets determined by including the data with reduced proton beam energy into a fit with the HERAPDF1.0 settings (right).

settings as used for HERAPDF1.0. The resulting PDFs are in agreement with the HERAPDF1.0 set (fig. 1 right). However, if only cross section measurements for $Q^2 > 5\,\mathrm{GeV}^2$ are used in the fit (a procedure included in the model uncertainty of HERAPDF1.0) the resulting gluon density shows a stronger rise towards low x.

At large Q^2 the cross section measurement for neutral current (NC) and charged current (CC) deep-inelastic scattering processes profits from the increased statistics in the HERA II running, especially for $e^- p$ scattering. H1 presents new results for the inclusive reduced cross section for NC and CC scattering in polarised $e^+ p$ and $e^- p$ collisions in the region $Q^2 > 200\,\mathrm{GeV}^2$ and $y < 0.9$. The data sets with opposite polarisation are also combined and corrected to unpolarised cross sections. Combined with the HERA I data, the NC data span five (four) orders of magnitude in Q^2 (x), respectively (fig. 2 left). They are well described by a PDF fit to the HERA I data of the H1 experiment, H1PDF2009 [2].

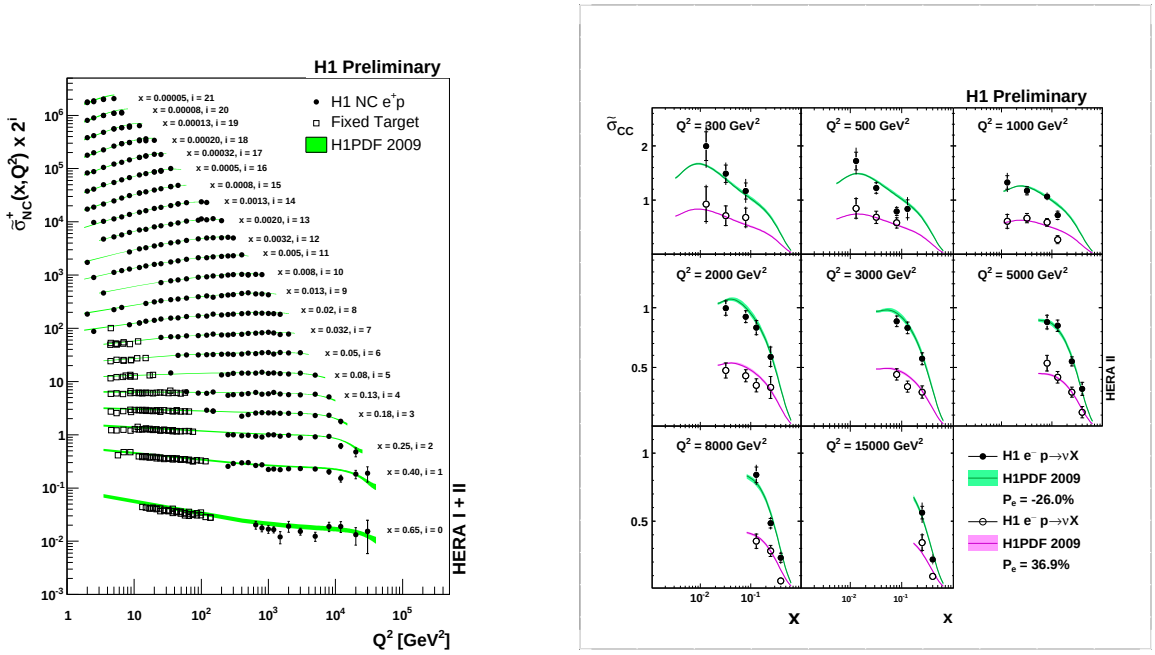

Figure 2: Inclusive reduced cross section for unpolarised neutral current $e^+ p$ scattering (left) and for polarised charged current $e^- p$ scattering (right).

Due to the absence of right-handed weak currents, the polarisation dependence of the CC cross section is expected to be linear and to vanish at $P_e = +1$ ($P_e = -1$) for $e^- p$ ($e^+ p$) scattering. The CC data show the expected large polarisation dependence (fig. 2 right) and can help to further constrain the valence quark distribution at large x. The measured total CC as a function of P_e is consistent with the expected linear behaviour (fig. 3 left). In NC scattering the polarisation dependence originates from the γZ interference. Figure 3 (right) shows the polarisation asymmetry for NC $e^+ p$ and $e^- p$ scattering. As for the unpolarised case, the predictions based on PDF sets determined from HERA I inclusive data describe the polarisation dependence of both the CC and the NC cross sections well.

A combined fit of the electroweak parameters and the proton PDFs has been performed to the inclusive cross sections at high Q^2 to determine the couplings of the Z boson to the u and the d

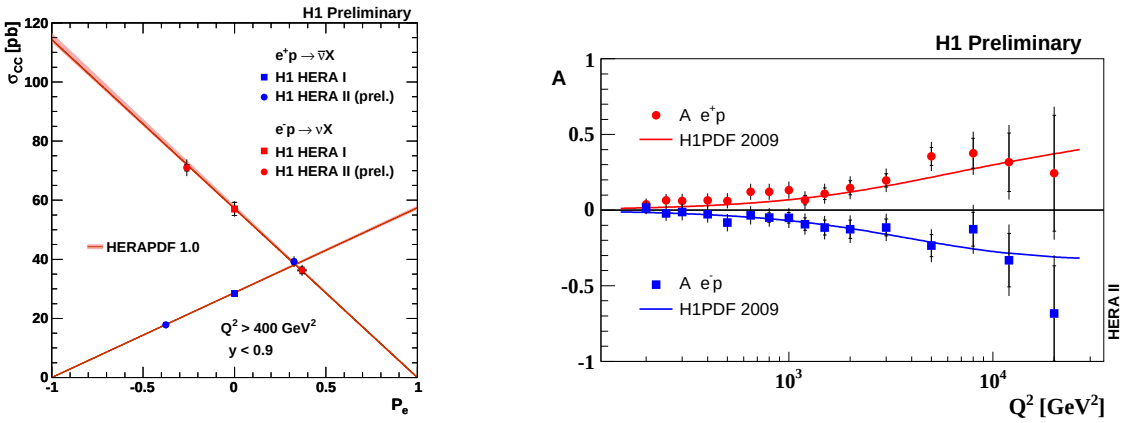

Figure 3: Polarisation dependence of the high Q^2 charged current data (left) and polarisation asymmetry of the neutral current data as a function of Q^2 (right).

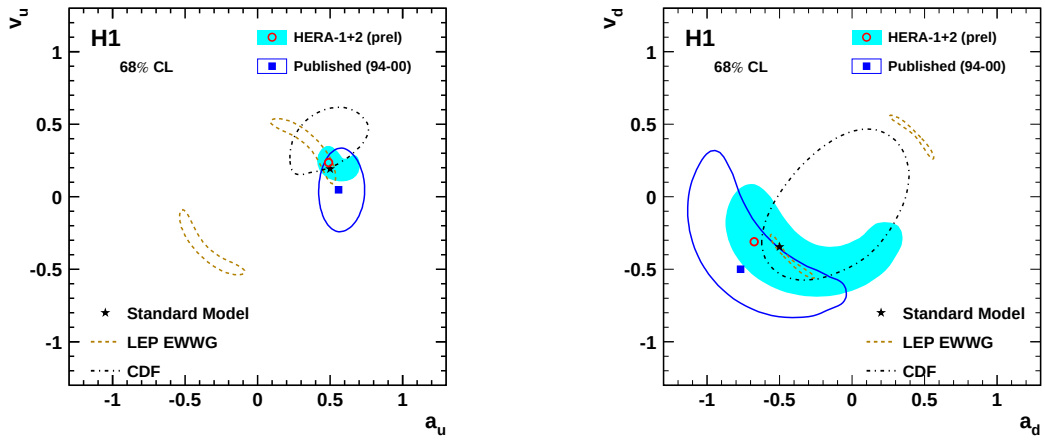

Figure 4: Vector and axial-vector couplings of the Z boson to u (left) and d (right) quarks determined in a combined electroweak and QCD fit to the H1 inclusive NC and CC data with polarised lepton beams.

quark. Apart from the increased statistics at HERA II this analysis profits from the polarisation of the lepton beams. This leads to a significant improvement in the precision of the vector coupling to the u quark (fig. 4).

3. QCD tests with the hadronic final state

The production of jets in deep-inelastic scattering at HERA offers a clean environment to test perturbative QCD calculations for the hadronic final state and to determine the scale dependence of the strong coupling α_S over a large range with a single experiment. Figure 5 (left) shows the cross section of inclusive jet production and of 2-jet and 3-jet events in the Breit frame in the low Q^2 region $5 < Q^2 < 100\,\mathrm{GeV}^2$ as a function of the jet transverse momentum $\langle P_T \rangle$ and of Q^2.

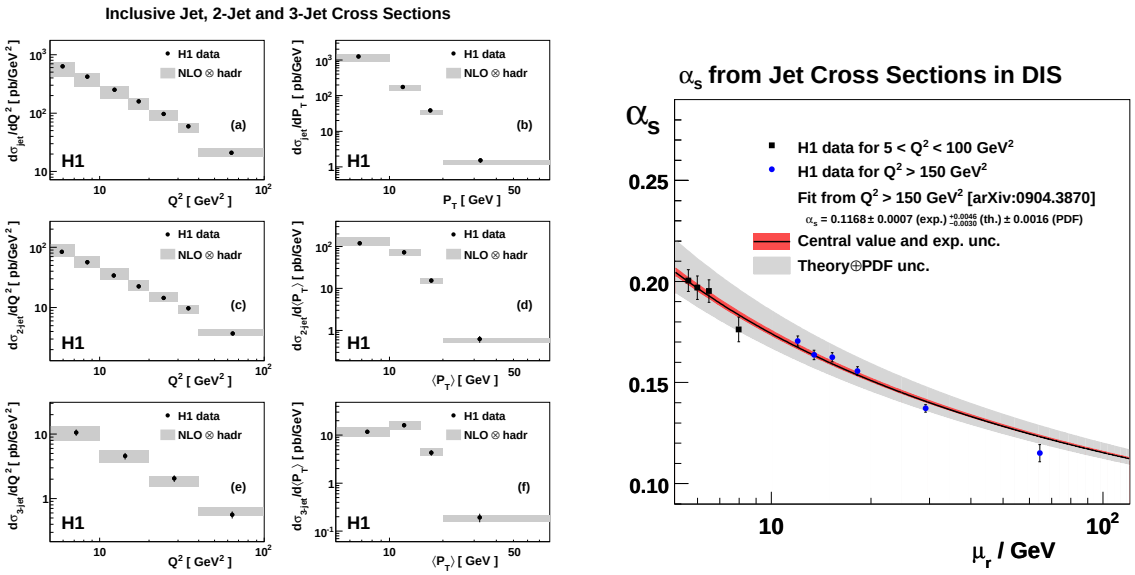

Figure 5: Cross section for inclusive jet, 2-jet and 3-jet production in the Breit frame at low Q^2 as a function of the jet transverse momentum and of Q^2 (left). Running of α_S as determined from jet production cross sections at low Q^2 and jet rates at high Q^2 (right).

The strong coupling constant is determined in an NLO QCD analysis to be $\alpha_S(M_Z) = 0.1160 \pm 0.0014(exp.)^{+0.0093}_{-0.0077}(th.) \pm 0.0016(PDF)$, in very good agreement with a previous measurement from jet rates at higher Q^2 [4]. Both measurements together can be used to demonstrate the running of the strong coupling in a wide range of the scale $\mu_r = \sqrt{(Q^2 + \langle P_T \rangle^2)/2}$ (fig. 5 right).

In the production of charm and beauty jets in DIS the mass of the heavy quark provides a third hard scale in addition to P_T and Q^2. The description of the data by an NLO pQCD calculation and the influence of the choice of scale is investigated by measuring the charm and beauty jet cross section in the laboratory and the Breit frame of reference. The heavy flavours are identified with a lifetime technique. The beauty jet cross section is well described by the NLO calculations where the latter exhibit only little dependence on the choice of scales (fig. 6 left). In case of charm jet production the predictions using a scale $\mu = \sqrt{Q^2 + 4M^2}$, with the heavy quark mass M, agree with the data, while they understimate the data at low transverse momenta with a scale choice of $\mu = \sqrt{(Q^2 + E_T^2 + M^2)/2}$ (fig. 6 right).

While the jet cross section measurements have only restricted sensitivity to the details of the parton evolution, the study of transverse momentum spectra of particles is better suited to distinguish DGLAP evolution, which has a strong k_T ordering in the parton cascade, from non-ordered parton emissions. At low transverse momentum p_T^* in the hadronic center-of-mass frame the distribution is expected to be dominated by fragmentation effects, while the parton evolution plays a significant role at larger p_T^*. As shown in fig. 7 (left), the measurement of the transverse momentum spectrum of charged particles at low Q^2 is better described by the DJANGOH Monte Carlo model, implementing unordered parton emission, than by the RAPGAP program based on DGLAP evolution. The CASCADE Monte Carlo uses the CCFM evolution equations and is close to the data only at the largest p_T^* studied.

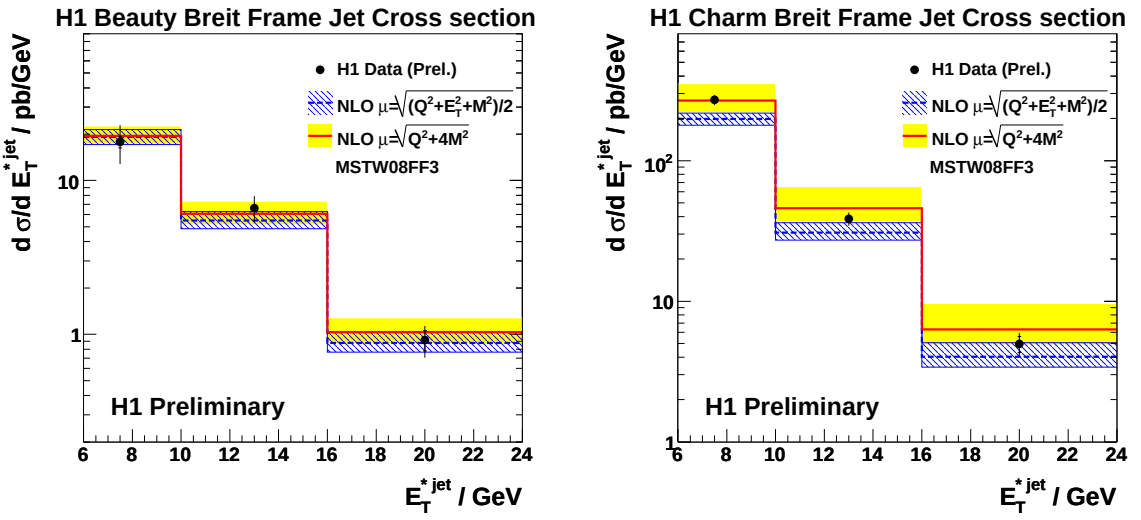

Figure 6: Cross section of beauty (left) and charm (right) jet production in DIS as a function of the jet transverse momentum in the Breit frame.

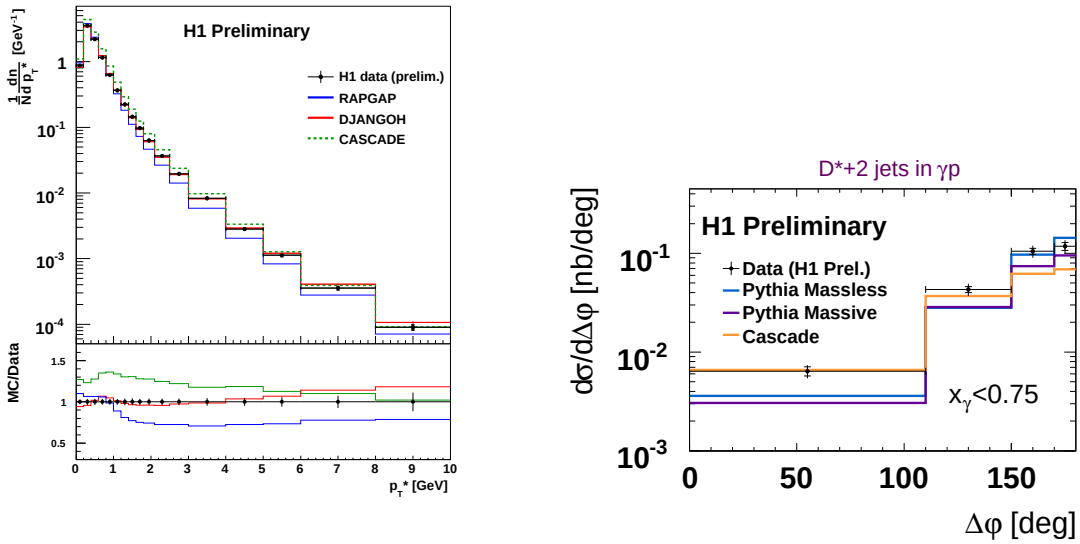

Figure 7: Transverse momentum spectrum of charged particles in the hadronic center-of-mass frame in low Q^2 DIS events (left). Azimuthal correlation of charm jets in photoproduction (right). The data are compared to Monte Carlo models implementing different parton dynamics.

Parton dynamics can also be investigated in jet correlations in multi-jet events. In the photoproduction of charm di-jets, tagged by the reconstruction of a D^* meson, variables sensitive to the parton dynamics are studied in two regions of phase space: $x_\gamma < 0.75$ enriched in resolved photon processes and $x_\gamma > 0.75$ enriched in direct processes. The difference in azimuth between the two jets $\Delta\phi$ at low x_γ is decribed neither by a MC based on DGLAP evolution (PYTHIA) nor by the CCFM Monte Carlo CASCADE (fig. 7 right).

4. Diffraction

Diffractive interactions are characterized by the fact that the scattered proton either stays intact (elastic scattering) or dissociates into a system with low mass M_Y (proton dissociation). Diffractive processes contribute to about 10% to the inclusive DIS cross section at HERA. They can be described by the exchange of an object with the quantum numbers of the vacuum. Experimentally diffraction can be detected by measuring the scattered proton or by requiring a large rapidity gap (LRG) with no hadronic activity close to the proton direction. The first method is free of proton dissociation, but limited in acceptance, while the second receives a proton dissociation contribution and is usually measured for the range $M_Y < 1.6\,\mathrm{GeV}$. New results for the LRG method and for scattered protons detected in the Forward Proton Spectrometer (FPS) or the Very Forward Proton Spectrometer (VFPS) are presented.

The diffractive reduced cross section is measured with the H1 data taken in the period 1999-2007 based on the LRG method in the region $3.5 < Q^2 < 90\,\mathrm{GeV}^2$, $x_{I\!P} < 0.05$ in fractional proton longitudinal momentum loss and $|t| < 1\,\mathrm{GeV}^2$ in squared four-momentum transfer at the proton vertex. An example for three selected β values, where $\beta = x/x_{I\!P}$, in one $x_{I\!P}$ bin is shown in fig. 8 (left) as a function of Q^2. The new data have much smaller statistical uncertainties than the previous H1 measurement. The two measurements are combined to one dataset for best precision.

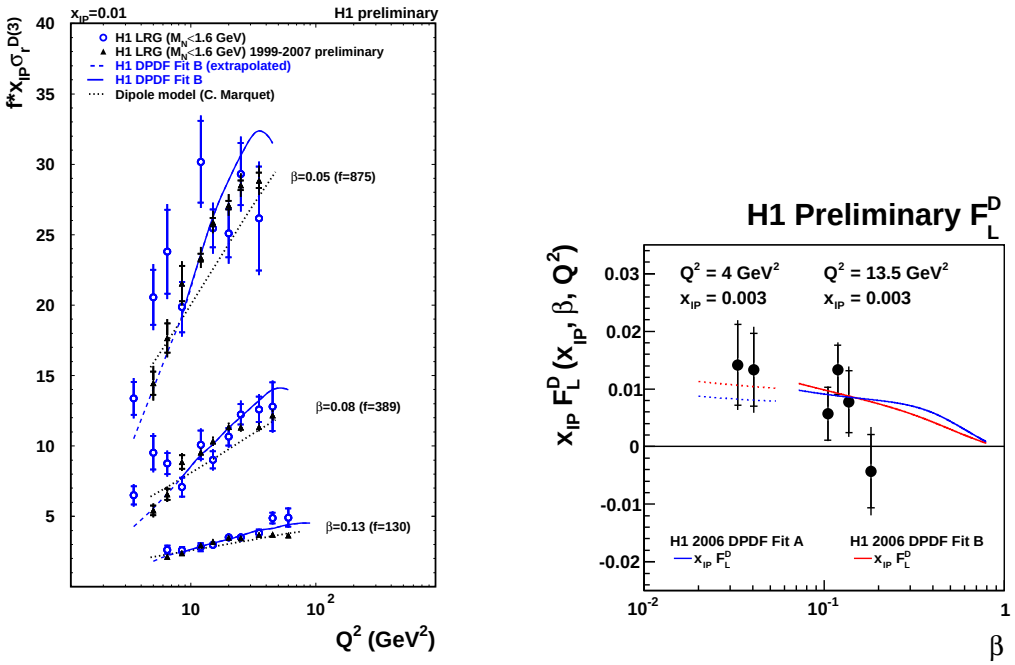

Figure 8: Examples for the diffractive reduced cross section measured with the LRG method (left). Diffractive longitudinal structure function F_L^D determined from LRG data in two Q^2 regions (right).

The large statistics in the LRG methods allows the extraction of the diffractive longitudinal structure function F_L^D from diffractive cross sections measured with different proton beam energies.

The new preliminary measurement extends to lower Q^2, where lower β are accessible (fig. 8 right). It confirms that F_L^D is non-zero and agrees with predictions based on fits of diffractive PDFs to the diffractive reduced cross section in LRG HERA I data.

The detection of the scattered proton offers the possibility to measure also t that is not accessible by the LRG method. A new measurement of the four-dimensional diffractive reduced cross section $\sigma_r^{D(4)}(\beta, Q^2, x_{IP}, t)$ is measured in three bins of $|t|$ (fig. 9). The x_{IP} and t dependences of the data can be described using a model which is motivated by Regge phenomenology, in which a leading pomeron and a sub-leading exchange contribute and proton vertex factorization is assumed.

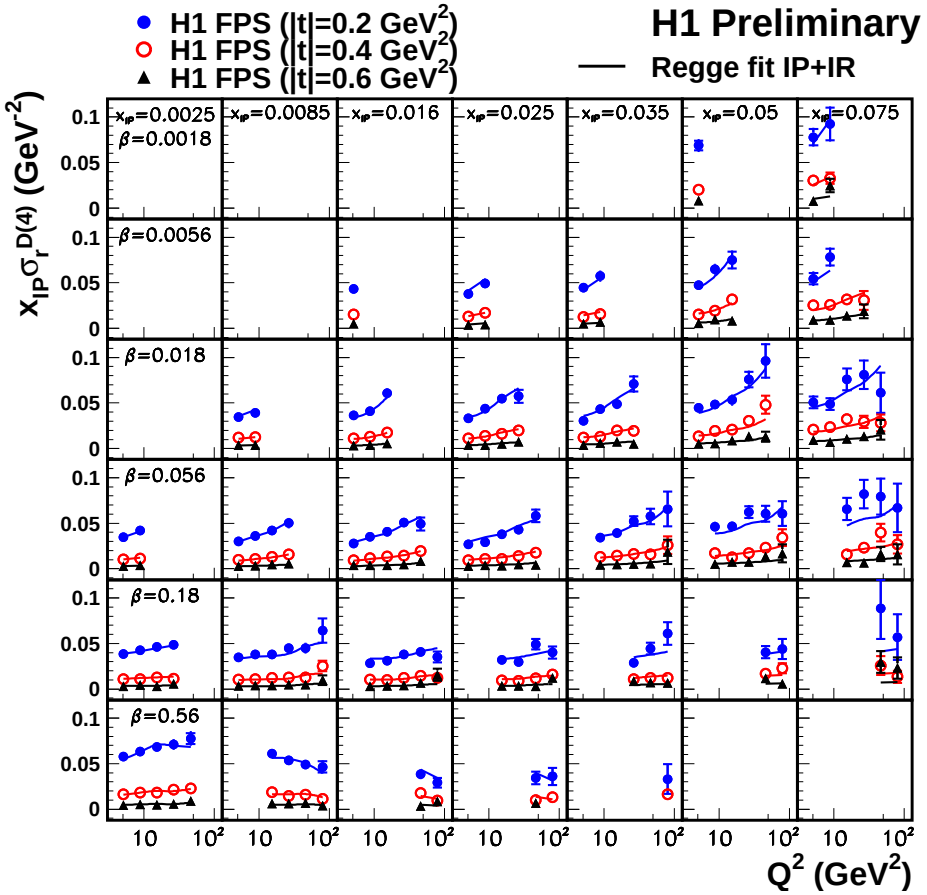

Figure 9: Four-dimensional diffractive reduced cross section $\sigma_r^{D(4)}(\beta, Q^2, x_{IP}, t)$ measured in 3 bins of $|t|$ with the H1 Forward Proton Spectrometer FPS. The solid curves represent the results of a phenomenological Regge fit to the data, including both the pomeron (IP) and a sub-leading (IR) exchange.

At HERA II the H1 detector was supplemented by the VFPS which allows the measurement of scattered protons in the range $0.009 < x_{IP} < 0.025$ with very high acceptance $> 90\%$. The first measurement of the inclusive diffractive reduced cross section $\sigma_r^{D(3)}(\beta, Q^2, x_{IP})$ with the VFPS is presented. The large acceptance and good resolution of the scattered proton momentum of the VFPS allow a fine binning in x_{IP}. The cross section is measured for $5 < Q^2 < 100\,\mathrm{GeV}^2$ and $0.005 < \beta < 0.8$. In the regions of overlap, the results agree well with the FPS and LRG mea-

surements after multiplying the latter by a factor 0.81 to take into account the proton dissociation contribution (fig. 10).

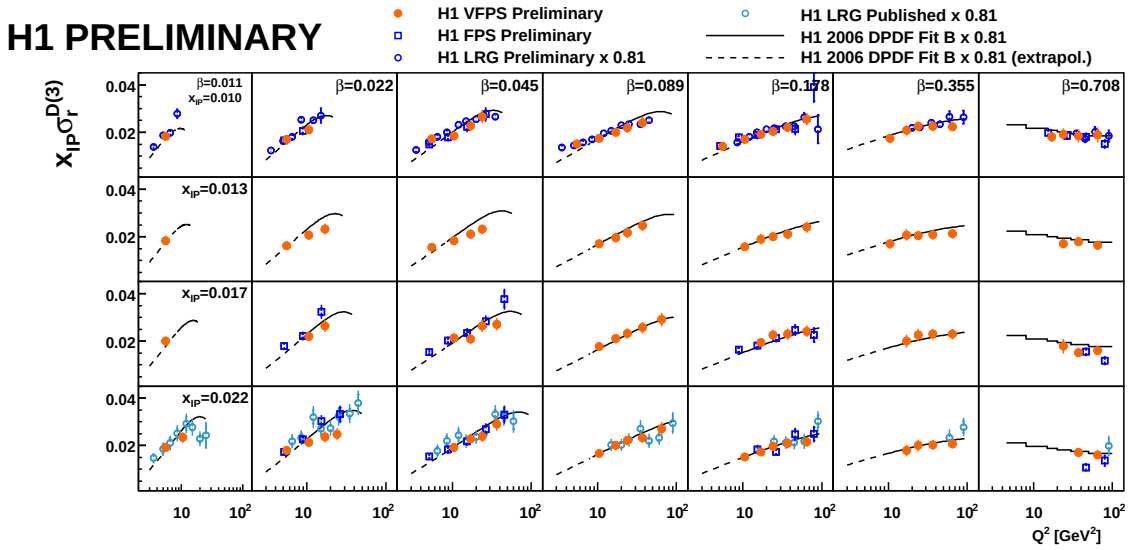

Figure 10: Inclusive diffractive reduced cross section $\sigma_r^{D(3)}(\beta, Q^2, x_{IP})$ measured with the H1 Very Forward Proton Spectrometer VFPS. The VFPS results are compared to independent measurements based on a scattered proton in the FPS and based on the LRG method (multiplied by a factor 0.81 to take into account the proton dissociation contribution).

5. Searches

A common extension of the Standard Model (SM) introduces a Supersymmetry between bosons and fermions. The R-parity R_p is then introduced to distinguish SM particles ($R_p = 1$) from their supersymmetric partners ($R_p = -1$). If R-parity is violated, single squarks can be produced resonantly in ep collisions. A new preliminary analysis of all relevant decay topologies using the complete H1 data set finds no deviation from the SM expectation. Exclusion limits at 95% confidence level (CL) are derived in the framework of the unconstrained Minimal Supersymmetric Standard Model and for the minimal Supergravity model (fig. 11). Squarks of all flavours up to masses of 275 GeV are excluded at 95% CL, assuming a coupling of electromagnetic strength ($\lambda = 0.3$).

A new search for the lepton flavour violating processes $ep \to \mu X$ and $ep \to \tau X$ was performed with the full H1 data set. This type of events could originate from the production or exchange of leptoquarks. Since no deviation from the SM expectation is found, limits on the coupling as a function of the leptoquark mass are derived for an extension of the Buchmüller-Rückl-Wyler model (fig. 12). For a coupling of electromagnetic strength masses up to 530 GeV (440 GeV) for leptoquarks decaying to a muon-quark (tau-quark) pair can be excluded at 95% CL.

The H1 and ZEUS collaborations performed a combined analysis in a common phase space to study events with an isolated lepton (e or μ) and missing transverse momentum [5]. In the SM these events can originate from the production of a single W boson. At large transverse momentum of the

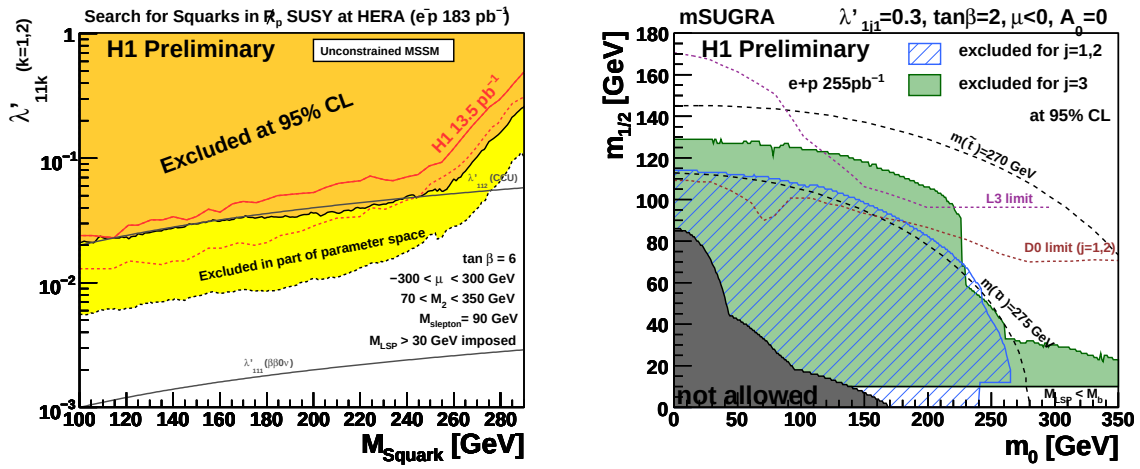

Figure 11: Limits at 95% CL on the production of squarks in *R*-parity violating Supersymmetry. Limits on the coupling as a function of the squark mass in the unconstrained Minimal Supersymmetric Standard Model (left) and in the $m_0, m_{1/2}$ plane for the minimal Supergravity model (right).

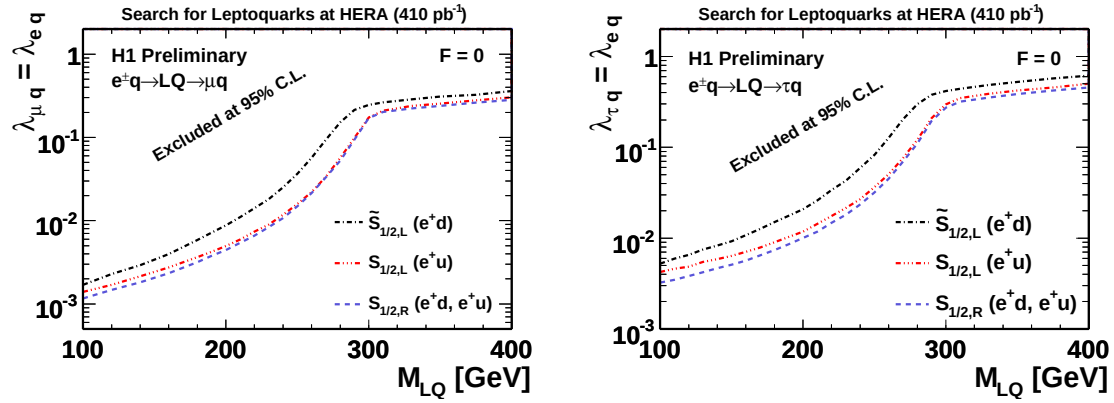

Figure 12: Exclusion limits at 95% CL for the coupling as a function of the leptoquark mass for scalar leptoquarks with fermion number $F = 0$ for second (left) and third (right) generation leptoquarks.

hadronic system $P_T^X > 25\,\text{GeV}$ an excess of data over the SM was reported in the H1 analysis for the e^+p data. Now in the combined analysis 23 events are observed compared to a SM prediction of 14.0 ± 1.9 (fig. 13 left). The data show a jacobian peak at the W mass in the transverse mass distribution of the lepton and the neutrino candidate reconstructed from the missing transverse momentum (fig. 13 middle). The cross section for single W production at HERA is measured as a function of P_T^X (fig. 13 right), and the total W cross section of $1.06 \pm 0.16(stat.) \pm 0.07(sys.)$ pb is found to be in good agreement with the SM expectation of 1.26 ± 0.19 pb.

Events with several high P_T leptons (e or μ) are also investigated in a combined analysis by H1 and ZEUS [6]. Within the SM such events are predominantly produced from photon-photon collisions. The yields of di-lepton and tri-lepton events are in good agreement with the SM predictions. At large transverse momentum the SM cross section is very small so processes beyond the SM could become visible. Seven events in e^+p collisions have a large scalar sum of the lepton trans-

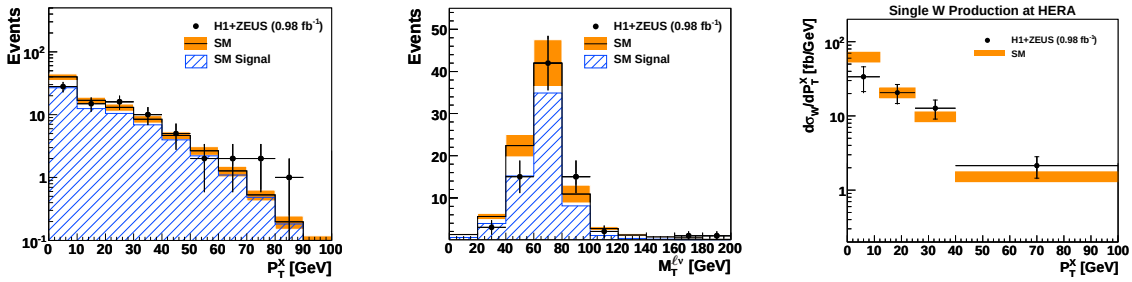

Figure 13: Distribution of the transverse momentum of the hadronic system P_T^X (left) and the transverse mass of the lepton and the neutrino candidate $M_T^{l\nu}$ (middle) for events with an isolated leptons and missing transverse momentum. Differential cross section for single W production as a function of P_T^X (right).

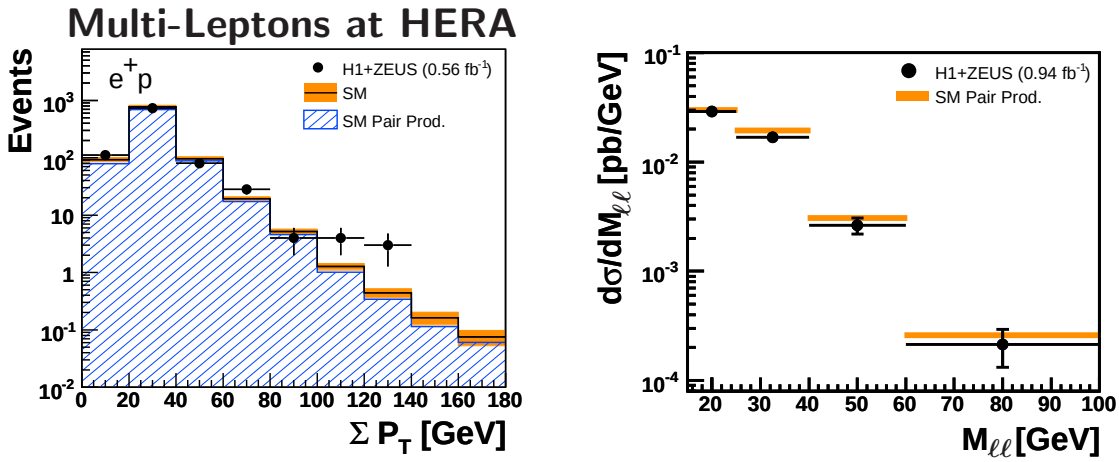

Figure 14: Distribution of the scalar sum of the transverse momenta of the leptons $\sum P_T$ in multi-lepton events (left). Differential cross section for leton pair production in photon-photon collisions as a function of the invariant mass of the leptons (right).

verse momenta $\sum P_T > 100\,\text{GeV}$, whereas the corresponding SM expectation is 1.94 ± 0.17 (fig. 14 left). The lepton pair production cross section in a photoprduction region dominated by photon-photon collisions is also measured and found to be described by the SM expectation (fig. 14 right). The total cross section of $0.66 \pm 0.03 \pm 0.03\,\text{pb}$ is in good agreement with the SM prediction of $0.69 \pm 0.02\,\text{pb}$.

6. Conclusions

A wealth of new results from the H1 experiment in the key areas of the H1 physics program was presented. The investigation of the structure of the proton profits from the increased statistics in the HERA II running phase especially at high Q^2, where new results for neutral current and charged current processes with polarised lepton beams were shown. The hadronic final state is used to test perturbative QCD calculations, study the parton dynamics in the proton and to determine the strong coupling α_S. New measurements of the diffractive structure functions with different experimental methods show good agreement and provide a coherent picture of diffraction. Most searches for

physics beyond the Standard Model are completed. In order to fully exploit the HERA potential and to achieve the final precision, H1 and ZEUS have started to combine their measurements.

7. Remarks

I would like to thank the organizers for their hard work to make the conference a success despite of all the problems arising from the volcano ashes. I was rather lucky to be able to arrive in time by train, in just two trains from Hamburg to Munich and from Munich to Firenze, and even getting hold of a place in a couchette.

References

[1] F. D. Aaron *et al.* [H1 Collaboration and ZEUS Collaboration], JHEP **1001** (2010) 109 [arXiv:0911.0884 [hep-ex]].

[2] F. D. Aaron *et al.* [H1 Collaboration], Eur. Phys. J. C **64** (2009) 561 [arXiv:0904.3513 [hep-ex]].

[3] F. D. Aaron *et al.* [H1 Collaboration], Eur. Phys. J. C **67** (2010) 1 [arXiv:0911.5678 [hep-ex]].

[4] F. D. Aaron *et al.* [H1 Collaboration], Eur. Phys. J. C **65** (2010) 363 [arXiv:0904.3870 [hep-ex]].

[5] F. D. Aaron *et al.* [H1 Collaboration and ZEUS Collaboration], JHEP **1003** (2010) 035 [arXiv:0911.0858 [hep-ex]].

[6] F. D. Aaron *et al.* [H1 Collaboration and ZEUS Collaboration], JHEP **0910** (2009) 013 [arXiv:0907.3627 [hep-ex]].